



3D Nanoweb of Zeolitic Imidazole Framework in Microfluidic System for Catalytic Applications

Journal:	<i>Reaction Chemistry & Engineering</i>
Manuscript ID	RE-ART-01-2020-000004.R1
Article Type:	Paper
Date Submitted by the Author:	13-Mar-2020
Complete List of Authors:	Ko, Dong-Hyeon; Pohang University of Science and Technology, Chemical Engineering Chen, Rui; Hanyang University Sun, Dengrong; Pohang University of Science and Technology Leem, Jin Woo; Hanyang University Joo, Jeong-Un; Pohang University of Science and Technology Kang, Il-Suk; Korea Advanced Institute of Science and Technology (KAIST), National Nanofab Center Sung, Myung Mo; Hanyang University, Chemistry Lee, Haiwon; Hanyang University, Department of Chemistry Kim, Dong-Pyo; Pohang University of Science and Technology, chemical engineering

ARTICLE

3D Nanoweb of Zeolitic Imidazole Framework in Microfluidic System for Catalytic Application†

Received 00th January 20xx,
Accepted 00th January 20xx

Dong-Hyeon Ko,^{‡a} Rui Chen,^{‡b} Dengrong Sun,^{‡a} Jin Woo Leem,^d Jeong-Un Joo,^a Il-Suk Kang,^c Myung Mo Sung,^d Haiwon Lee^{*bd} and Dong-Pyo Kim^{*a}

DOI: 10.1039/x0xx00000x

3D nanoweb-like zeolite imidazole framework (ZIF-8) as an efficient heterogeneous catalyst was structured inside a functionalized microfluidic channel by immobilizing the ZIF on 3D carbon nanotubes (CNTs) network across the gap among the built-in micropillars for the Knoevenagel condensation reaction. The quantitative conversion was achieved under mild conditions of ethanol solvent and room temperature. The ZIF-8 3D nanoweb systems showed higher conversion than the identical systems without CNTs-based networks which indicate the catalytic superiority of 3D nanoweb structures.

Introduction

Microfluidic reaction system, containing open paths for fluids with sub-millimeter dimension called microchannels, has been regarded as an enhanced alternative for traditional synthetic tools represented by the round-bottomed flask, owing to its increased surface to volume ratio.¹⁻³ Utilization of heterogeneous catalysts, especially with immobilization technique, is a well-precedented option for synthetic chemistry in the microfluidic reaction system and has been thoroughly studied in the view of a full-contact of reactants to catalytic active sites in confined space.⁴⁻¹⁷

For instance, Zhang *et al.* reported a strategy of immobilizing silver nanoparticle catalysts on the walls of the microfluidic reaction system.⁷ The immobilized silver nanoparticles not only showed superior catalytic activities for a reduction reaction but also good stabilities after long-term uses. Uozumi *et al.* reported a strategy to form a catalytic polymer membrane of a palladium complex inside a microchannel by utilizing polymer deposition at a laminar interface.¹⁴ The catalytic palladium-complex membrane was utilized for the carbon-carbon bond-forming reactions of aryl halides and aryl boronic acids. Vishwakarma *et al.* reported an approach to immobilize ionic liquid catalysts on the interface of gas-liquid laminar flow with an aid of superamphiphobic silicon nanowires.¹⁷ By immobilizing ionic liquid catalysts on the tip of silicon

nanowires, the interfacial catalysis between the gas and liquid was feasible for *in situ* carbon dioxide capture and utilization.

However, despite the successful applications with various immobilization strategies including on-wall types,⁷⁻¹³ membrane types,^{6, 14-16} and interfacial types,^{17, 18} the microreaction systems are still challenging with the difficulties on the spatial positioning of the built-in microstructures on which heterogeneous catalysts are immobilized. Therefore, the reported researches have mostly attempted the planar or curved 2D spatial arrangement of heterogeneous catalysts. This inherently possesses limitations considering the contact between reactant molecules and catalysts.

The adoption of microstructures in the microchannel can enhance the efficiency of reaction by increasing the collisions between the reactants with repeated disturbance of reactant flow.^{19, 20} Among the microstructures, vertically aligned micropillar array in the microchannel,²¹⁻²³ whose height matches that of the microchannel, are easy to make but still effective static mixer structures. However, despite efforts from the embedded micropillar structures, most of the reactant molecules flow through the gap between the micropillars with their highest fluidic speed, and the gap is still too large from the point of view of reactant molecules.²⁴ Therefore, it is simply anticipated that the positioning of nanostructures as catalyst supporters across the gap between the micropillars may enhance the efficacy of microfluidic catalytic reaction to the ideal level.

Herein, we report on the microfluidic reaction system incorporated with 3D nanoweb-like zeolitic imidazole framework-8 (ZIF-8) catalysts on the carbon nanotube (CNT) networks that are grown across the built-in micropillars. The robust nanoweb-shaped CNT networks enable to stably support the immobilized ZIF-8 catalyst and to catalyze liquid-phase organic reactions under a fluidic flow (totally ~200 $\mu\text{L}/\text{min}$) of reactant liquids. The Knoevenagel condensation between benzaldehyde and malononitrile was performed as a model reaction to show the superiority of ZIF-8 3D nanoweb catalytic

^a Center for Intelligent Microprocess of Pharmaceutical Synthesis, Department of Chemical Engineering, Pohang University of Science and Technology (POSTECH), Pohang 37673, Korea.

^b Institute of Nano Science and Technology, Hanyang University, Seoul 04763, Korea.

^c National Nanofab Center, Korea Advanced Institute of Science and Technology (KAIST), Daejeon 34141, Korea.

^d Department of Chemistry, Hanyang University, Seoul 04763, Korea.

† Electronic Supplementary Information (ESI) available: Characterization of CNT strands, detailed design of the micropillar-embedded microchannel, SEM images of CNT networks and ZIF-8 catalysts, EDS results of ZIF-8, and schematic illustration of fabrication. See DOI: 10.1039/x0xx00000x

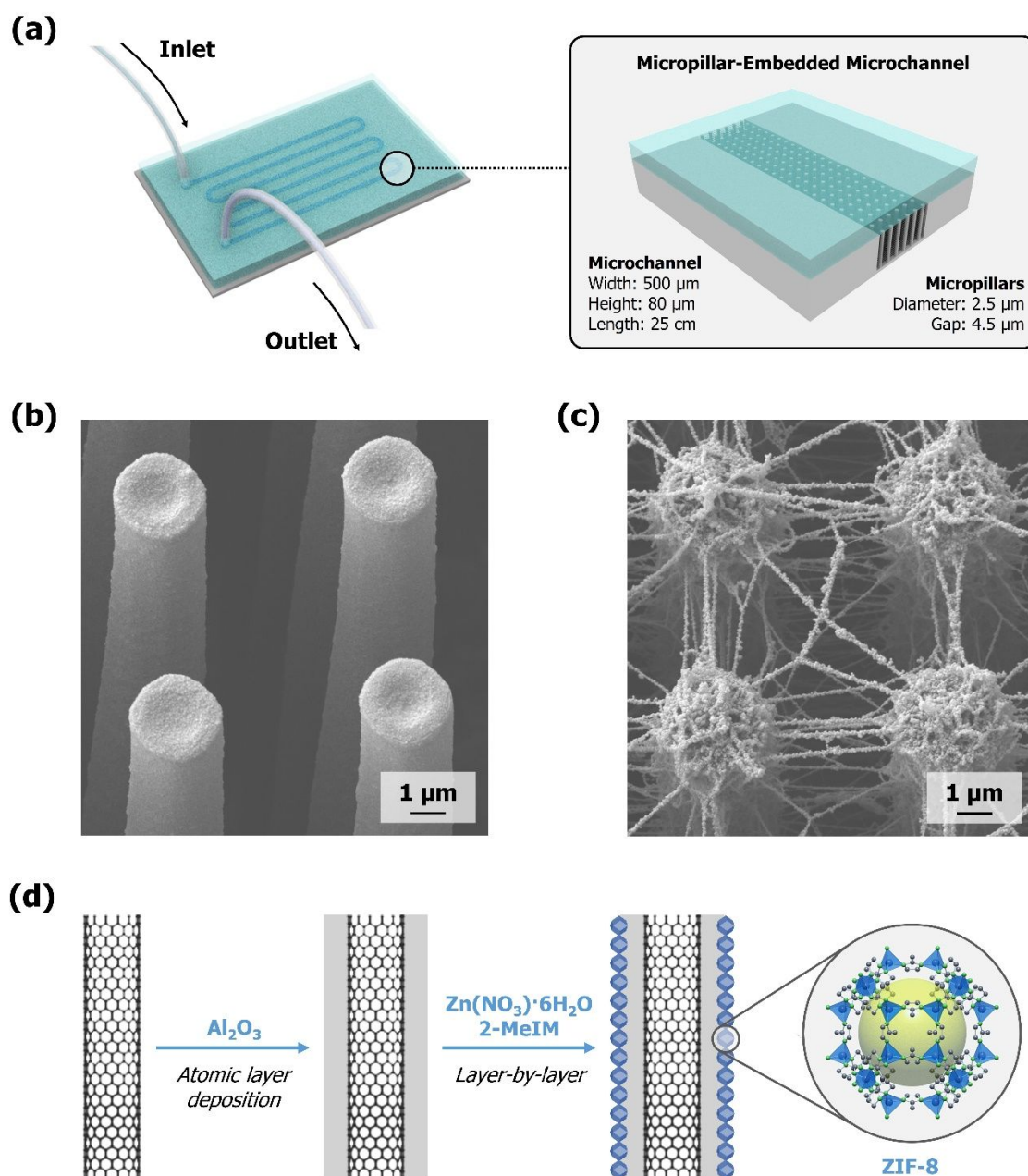


Figure 1. (a) Illustration of ZIF-8 3D nanoweb-embedded microfluidic reaction system. Scanning electron microscopy (SEM) images of zeolitic imidazole framework-8 (ZIF-8) catalysts on (b) micropillars embedded in the microchannel and (c) micropillars with CNT-based 3D networks after atomic layer deposition (ALD) coating embedded in the microchannel. (d) Schematic illustration of ZIF-8 immobilization on the CNT-based networks after ALD coating.

microfluidic system compared to the ZIF-8 only on the micropillar system.

Results and Discussion

Microfluidic reaction systems with embedded micropillars have been developed (Figure 1a) for heterogeneous catalysis. The microchannel with built-in micropillars was fabricated by silicon deep etching of p-type Si wafer. Computational fluid dynamics (CFD) simulation revealed that the fluid velocity is higher at free space between pillars than near the pillars due to steric resistance (Figure S1). For a comparative study, ZIF-8

catalysts were immobilized on the systems in the absence and presence of CNT-based 3D networks as shown in scanning electron microscope (SEM) images in Figure 1b and Figure 1c, respectively. The 3D networking of CNTs across the micropillars was conducted in the gas phase²⁵ after atomic layer deposition (ALD) of Al_2O_3 to enhance the mechanical strength of the network and to introduce amine functional groups on the surface.²⁶ Finally, ZIF-8 particles were grown on the CNT network in the liquid phase (Figure 1d).

The 3D network of CNTs is an excellent substrate to be a supporter for catalyst immobilization. The 3D networking of CNTs is mainly done by a vibratory growth with a swing of the

extended CNT from the surface of the micropillars and following nearest-neighbor interconnection.²⁷ The aspect of CNT networking is mainly affected by the gap between the micropillars. We found that from 4 to 5 μm is a suitable size of the gap for the microfluidic catalysis. The narrower gap of less than 3 μm led to the formation of many strands of CNTs in high density. Growth of ZIF-8 on those narrower micropillars led to a formation of a wall-like aggregation of ZIF-8 catalysts which was immoderate for fluidic flow owing to severe pressure drop in the microchannel. When the gap was larger than 6 μm , the network growth of CNTs across the gap was incomplete which leads to few and weak CNT-based networks (**Figure S2**). Alternatively, the height of the micropillar was fixed to be 80 μm since the taller micropillars rendered the non-uniform pillar shape along the column due to limited process control (**Figure S3**). Thus, a vertically aligned array of micropillars with a diameter of 2.5 μm , a height of 80 μm , and inter-micropillar gap of 4.5 μm was prepared by a deep Si etching process in the confined region of serpentine microchannel shape with a width of 500 μm and length of 25 cm (**Figure 1a** and **Figure S4**). A dense network of CNTs was observed across the 80- μm -height of micropillars (**Figure 1c**). The diameter of each CNT bundles after ALD coating was found to be *ca.* 50 nm (**Figure S5a**).

As a new subclass of metal-organic frameworks (MOFs), ZIFs have emerged due to their highly porous surfaces.²⁸ Most of the applications using ZIFs have been carried out in the field of gas separation.²⁹ Very recently, some studies have been performed on the catalytic performance of ZIFs.³⁰⁻³³ In spite of the researches to utilize ZIF catalysts in microfluidic systems, it still remained the challenge of expansion by macroscopic structuring of the ZIF crystals. In this context, a noble structure of ZIF-8 3D nanoweb is considered as an efficient tool for heterogeneous catalysis in microfluidic systems.

To immobilize ZIF-8 on the as-prepared CNTs-based networks as well as the micropillars, the layer-by-layer (LbL) method was exploited with the metal and ligand solutions (see Materials and Methods for the details).³⁴ The surfaces of CNTs and micropillars were modified with polyvinylpyrrolidone (PVP) to control nucleation and growth of ZIF-8 crystals by flowing the PVP in methanol solution into the microfluidic system for 3 h,³⁵ and following LbL process was performed by feeding the metallic and the ligand precursor solutions in an alternating manner. The uniform decoration of ZIF-8 crystals on CNT networks was confirmed by SEM image and XRD analysis (**Figure 1c** and **Figure S6**). The energy dispersive spectroscopy (EDS) further proved the formation of ZIF-8 crystals on Al_2O_3 -coated CNT networks (**Figure S7**) with 28.55 wt% zinc, 18.41 wt% aluminum, 38.21 wt% carbon, 12.07 wt% oxygen and 2.76 wt% Si. To fabricate a comparative system, ZIF-8 immobilization on the micropillars without the CNT network in the microchannel was also carried out under the identical condition, as observed (**Figure 1b** and **Figure S8**).

The Knoevenagel condensation between aldehydes and the compounds with activated methylene group is a widely applied carbon-carbon bond-forming mechanism.³⁶ The reaction was comparatively performed by separately injecting two reagents of benzaldehyde and malononitrile diluted in ethanol into two

microfluidic systems: ZIF-8 immobilized on 3D CNT nanoweb, ZIF-8 on micropillar system. (see Materials and Methods for the details) at room temperature.

Two reaction systems showed different efficiency in the conversion of the Knoevenagel condensation. The ZIF-8 3D nanoweb microfluidic reaction system gave 55 % at 3.5 s of retention time and 96 % at 12 s, whereas the system with ZIF-8 on micropillar reached only 10 % at 3.5 sec and 75 % at 12 s of the residence time (**Figure 2**). Finally, the micropillar system without CNT networks needed 35 s to obtain the full conversion, which took much longer than 17.5 s of the ZIF-8 3D nanoweb system. The superior reaction performance of ZIF-8 3D nanoweb to the batch as well as to the simple pillar system is the most likely attributed to the larger amount of ZIF-8 catalyst loading on the increased surface area of homogeneously suspended CNT, facilitating the access of substrates into catalyst (**Table S1**). It is well known that the pressure-driven flow in the microchannel caused a parabolic profile of fluid velocity, generally resulting in nearly zero flow velocity around the wall under ordinary slip condition.³⁷ This implies that the immobilized catalysts in planar arrangement have a less chance to meet the reagents, the reactant molecules need some diffusion time to reach the catalyst on the supporters.

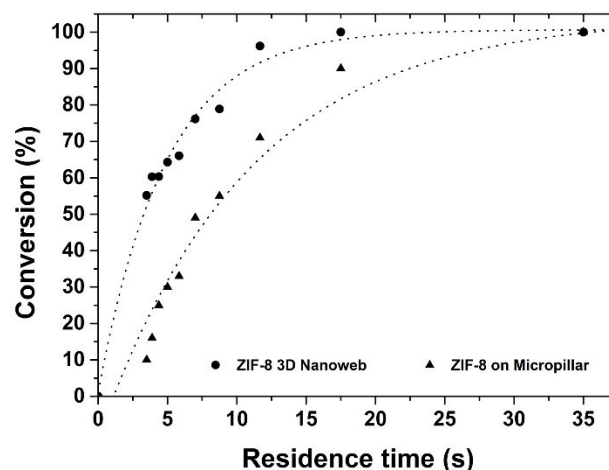


Figure 2. Synthetic conversions (based on benzaldehyde) at different residence times for Knoevenagel condensation between benzaldehyde and malononitrile in ethanol at room temperature. Circles (●) and triangles (▲) indicate the catalytic reaction of ZIF-8 3D nanoweb microfluidic system, ZIF-8 on micropillar system without CNT networks, respectively. Insets indicate each heterogeneous catalysis system inside the microfluidic reaction systems.

Materials and Methods

Preparation of the 3D network of CNTs on Micropillar embedded in Microchannel

The 3D network of CNTs was synthesized on micropillars by following the reported method. The micropillars were made on a confined region of 8-inch p-type Si (1 0 0) wafer by silicon deep etching process.³⁸ The confined region had a serpentine shape

(width: 500 μm , length: 25 cm) which is within a rectangular unit (5 cm x 3 cm) on the Si wafer. The micropillars with a diameter of 2.5 μm , a height of 80 μm , and an inter-micropillar gap of 4.5 μm were prepared within the confined region with the in-line arrangement, which is called micropillar-embedded microchannel. The Si wafer substrate with micropillar-embedded microchannel was soaked in a piranha solution ($\text{H}_2\text{SO}_4\text{:H}_2\text{O}_2 = 7\text{:}3$) for 3 h for cleaning and surface-modification with a hydroxyl group. After the treatment, the substrate was fully rinsed with DI water followed by drying with nitrogen gas. 0.404 g of $\text{Fe}(\text{NO}_3)_3 \cdot 9\text{H}_2\text{O}$ and 1.37 mL of Mo in NH_4OH solution was dissolved in 50 mL of ethanol by ultrasonication to make a catalyst solution.²⁵ The piranha-treated substrate was dipped in the catalyst solution for 2 h and subsequently dipped in ethanol for 10 min for removal of excess Fe/MO catalyst. The 3D network of CNTs was synthesized by a thermal chemical vapor deposition method.³⁹ The substrate was placed in a quartz tube reactor and the reactor was heated up to 800 $^\circ\text{C}$. After the reactor's temperature reached 800 $^\circ\text{C}$, NH_3 gas (300 sccm) was introduced into the reactor for 10 min followed by C_2H_2 gas (10 sccm) for 20 min. The as-prepared samples with 3D networks of CNTs were cooled down to room temperature. The networked CNTs were coated with Al_2O_3 by using the ALD method to enhance the mechanical strength and to modify the surface with amine functional groups.²⁶

Preparation of CNT-networked Microfluidic System

A polydimethylsiloxane (PDMS) slab with a thickness of 0.5 mm, on which two holes for inlet and outlet were punched with a diameter of 1.5 mm, was used as an upper part of the microfluidic system. The PDMS slab was bonded to the substrate with CNT-networked microchannel by positioning two holes directly on each end of the CNT-networked microchannel. PDMS precursor solution was used for strong and homogeneous bonding between the PDMS slab and the microchannel substrate with a modified method inspired by the microcontact printing method (Figure S9).⁴⁰ PDMS precursor solution mixed at 10:1 curing ratio was degassed and spin-coated on 3-inch Si wafer at 6,000 rpm for 30 s. The PDMS slab was treated with oxygen plasma for 1 min and gently placed on the spin-coated thin layer of PDMS precursor solution to make the plasma-treated surface to contact the precursor solution. After a few seconds, the precursor solution was fully immersed on the surface of the PDMS slab. The PDMS slab with uncured PDMS precursor layer was then aligned on the substrate with CNT-networked microchannel and the PDMS precursor layer was cured by heating them at 70 $^\circ\text{C}$ for 2 h. Connection of PTFE tubings on inlet and outlet was followed to finish making the microchannel system (Figure 1a).

With the adopted bonding method, the PDMS slab and the substrate with CNT-networked microchannel showed secure bonding even with water flowing test through the microchannel with a high flow rate up to 100 $\mu\text{L}/\text{min}$ for 60 min. It was also confirmed by SEM that after the water flowing test with the flow rate of 100 $\mu\text{L}/\text{min}$ for 20 min the 3D network of CNTs remained intact without any damage (Figure S5b).

Preparation of ZIF-8 3D Nanoweb-embedded Microfluidic Reaction System

The as-made microfluidic system was turned into a ZIF-8-immobilized microfluidic reaction system by synthesizing ZIF-8 on the 3D network of ALD treated CNTs by LbL synthesis method.³⁴ PVP in methanol solution (2 mg/mL) flowed into the microfluidic system at a flow rate of 10 $\mu\text{L}/\text{min}$ for 3 h to control the growth of ZIF-8.³⁵ A pure methanol flowed into the system at the same flow rate for 5 min. 2-MeIM in methanol solution (0.35 mg/mL) and $\text{Zn}(\text{NO}_3)_2 \cdot 6\text{H}_2\text{O}$ in methanol solution (0.9 mg/mL) were prepared. A flow cycle consists of the flows of two solutions in 5 min for each was repeated 20 times. The flow of pure methanol was performed between changing the solution from each to each to wash out the excess of precursors. After the 20 cycles of LbL synthesis, the entire system was vacuum-dried overnight at 80 $^\circ\text{C}$. The synthesized nanoweb-shaped ZIF-8 crystals were characterized by SEM analysis.

Preparation of ZIF-8 on Si wafer for XRD analysis

The ZIF-8 on Si wafer was prepared following similar procedures as ZIF-8 3D nanoweb with slight modifications. Si wafer was treated with PVP in methanol solution (2 mg/mL) for 3 h. After washing with fresh methanol twice, the surface modified Si wafer was immersed in methanol solution of $\text{Zn}(\text{NO}_3)_2 \cdot 6\text{H}_2\text{O}$ (0.9 mg/mL) for 5 min. Subsequently, the methanol solution of 2-MeIM (0.35 mg/mL) was added. The vial was kept undisturbed overnight. The obtained ZIF-8 grown Si wafer was washed with methanol several times and dried for XRD analysis.

Catalytic Studies

The Knoevenagel condensation between benzaldehyde and malononitrile using the immobilized ZIF-8 as a catalyst was carried out both in the ZIF-8 3D nanoweb-embedded microfluidic reaction system and the comparative system without CNT network at room temperature.³⁰ Benzaldehyde in ethanol solution (5.3 mg/mL) and malononitrile in ethanol solution (3.3 mg/mL) were prepared. Both solutions contained in each syringe flowed in PTFE capillary tubings at a flow rate ranging from 10 to 100 $\mu\text{L}/\text{min}$ for each and was mixed using a micro-mixing tee. The mixed solution was immediately flowed into the microfluidic reaction systems by flowing in another short (~2 cm) capillary tubing. The solution flowed through the microchannel embedded with micropillars, 3D network of CNTs and ZIF-8 crystals on them. Another capillary tubing was connected to the outlet of the microfluidic reaction system, whose other end is connected to a vial containing 2 mL DI water for quenching the reaction. After collecting 400 μL of total product-containing solution for each flow rate (20 min for 10 $\mu\text{L}/\text{min}$ flow rate and 2 min for 100 $\mu\text{L}/\text{min}$ flow rate of each solution), 8 mL ethyl acetate was mixed to the 2 mL DI water mixed with the product-containing solution for extraction of product. The extracted product was measured by GC-MS to calculate and compare the conversions for each flow rate.

Conclusion

In summary, a novel microfluidic reaction system with embedded 3D nanoweb of ZIF-8 catalysts assisted by the carbon nanotube (CNT) networks has been presented. The inherent strength of CNT networks treated by the ALD process enables the high-flow-rate liquid-phase reactions with secure immobilization of ZIF-8. The results of the Knoevenagel condensation reveal the superiority of 3D nanoweb structuring of ZIF-8 in terms of heterogeneous catalysis. This truly 3D structuring of ZIF catalysts bodes well for liquid phase organic reactions catalyzed by heterogeneous catalysts which can be immobilized on the surface of CNTs.

Conflicts of interest

There are no conflicts to declare.

Acknowledgments

We gratefully acknowledge the support from the National Research Foundation (NRF) of Korea grant funded by the Korean government (2017R1A3B1023598, 2012R1A6A1029029). Funding was also provided by the grant (FA2386-15-1-4081) from the AFOSR/AOARD, USA. Authors appreciate the contribution of Sejun Yim for CFD work.

Notes and references

‡ These authors contributed equally.

1. K. S. Elvira, X. C. i Solvas, R. C. R. Wootton and A. J. deMello, *Nature Chemistry*, 2013, **5**, 905.
2. K. Geyer, J. D. C. Codée and P. H. Seeberger, *Chemistry – A European Journal*, 2006, **12**, 8434-8442.
3. J. Kobayashi, Y. Mori and S. Kobayashi, *Chem. Asian J.*, 2006, **1**, 22-35.
4. G. Jas and A. Kirschning, *Chemistry – A European Journal*, 2003, **9**, 5708-5723.
5. A. Tanimu, S. Jaenicke and K. Alhooshani, *Chemical Engineering Journal*, 2017, **327**, 792-821.
6. L. Cseri, T. Fodi, J. Kupai, G. T. Balogh, A. Garforth and G. Szekely, *Advanced Materials Letters*, 2017, **8**, 1094-1124.
7. L. Zhang, Z. Liu, Y. Wang, R. Xie, X.-J. Ju, W. Wang, L.-G. Lin and L.-Y. Chu, *Chemical Engineering Journal*, 2017, **309**, 691-699.
8. R. Wunsch, M. Fichtner, O. Görke, K. Haas-Santo and K. Schubert, *Chemical Engineering & Technology: Industrial Chemistry–Plant Equipment–Process Engineering–Biotechnology*, 2002, **25**, 700-703.
9. G. Zhang, T. Zhang, X. Zhang and K. L. Yeung, *Catalysis Communications*, 2015, **68**, 93-96.
10. H.-I. Ryoo, J. S. Lee, C. B. Park and D.-P. Kim, *Lab on a Chip*, 2011, **11**, 378-380.
11. B.-B. Xu, R. Zhang, X.-Q. Liu, H. Wang, Y.-L. Zhang, H.-B. Jiang, L. Wang, Z.-C. Ma, J.-F. Ku, F.-S. Xiao and H.-B. Sun, *Chemical Communications*, 2012, **48**, 1680-1682.
12. S. R. A. de Loos, J. van der Schaaf, M. H. J. M. de Croon, T. A. Nijhuis and J. C. Schouten, *Chemical Engineering Journal*, 2012, **179**, 242-252.
13. N. Wang, X. Zhang, Y. Wang, W. Yu and H. L. W. Chan, *Lab on a Chip*, 2014, **14**, 1074-1082.
14. Y. Uozumi, Y. M. A. Yamada, T. Beppu, N. Fukuyama, M. Ueno and T. Kitamori, *J Am Chem Soc*, 2006, **128**, 15994-15995.
15. M. Liu, X. Zhu, R. Chen, Q. Liao, H. Feng and L. Li, *Chemical Engineering Journal*, 2016, **301**, 35-41.
16. S. Kovačič, M. Mazaj, M. Ješelnik, D. Pahovnik, E. Žagar, C. Slugovc and N. Z. Logar, *Macromolecular Rapid Communications*, 2015, **36**, 1605-1611.
17. N. K. Vishwakarma, A. K. Singh, Y.-H. Hwang, D.-H. Ko, J.-O. Kim, A. G. Babu and D.-P. Kim, *Nature Communications*, 2017, **8**, 14676.
18. M. Zhang, L. Wei, H. Chen, Z. Du, B. P. Binks and H. Yang, *J Am Chem Soc*, 2016, **138**, 10173-10183.
19. T. W. Lim, Y. Son, Y. J. Jeong, D.-Y. Yang, H.-J. Kong, K.-S. Lee and D.-P. Kim, *Lab on a Chip*, 2011, **11**, 100-103.
20. A. Bertsch, S. Heimgartner, P. Cousseau and P. Renaud, *Lab on a Chip*, 2001, **1**, 56-60.
21. S. Tähkä, J. Sarfraz, L. Urvás, R. Provenzani, S. K. Wiedmer, J. Peltonen, V. Jokinen and T. Sikanen, *Analytical and Bioanalytical Chemistry*, 2019, **411**, 2339-2349.
22. L. Li, R. Chen, Q. Liao, X. Zhu, G. Wang and D. Wang, *International Journal of Hydrogen Energy*, 2014, **39**, 19270-19276.
23. B. Zhou, W. Xu, A. A. Syed, Y. Chau, L. Chen, B. Chew, O. Yassine, X. Wu, Y. Gao, J. Zhang, X. Xiao, J. Kosel, X. X. Zhang, Z. Yao and W. Wen, *Lab on a Chip*, 2015, **15**, 2125-2132.
24. W. Zhou, Q. Wu, H. Jiang and M. Zhu, 2011.
25. J. Seo, T. J. Lee, S. Ko, H. Yeo, S. Kim, T. Noh, S. Song, M. M. Sung and H. Lee, *Advanced Materials*, 2012, **24**, 1975-1979.
26. S. Lee, J. Lee, D. W. Lee, J.-M. Kim and H. Lee, *Chemical Communications*, 2016, **52**, 926-929.
27. Y. Homma, Y. Kobayashi, T. Ogino and T. Yamashita, *Applied Physics Letters*, 2002, **81**, 2261-2263.
28. A. Phan, C. J. Doonan, F. J. Uribe-Romo, C. B. Knobler, M. O'keeffe and O. M. Yaghi, *Accounts of Chemical Research*, 2010, **43**, 58-67.
29. D. Liu, X. Ma, H. Xi and Y. S. Lin, *Journal of Membrane Science*, 2014, **451**, 85-93.
30. U. P. N. Tran, K. K. A. Le and N. T. S. Phan, *ACS Catalysis*, 2011, **1**, 120-127.
31. L. T. Nguyen, K. K. Le, H. X. Truong and N. T. Phan, *Catalysis Science & Technology*, 2012, **2**, 521-528.
32. R. Jin, Z. Bian, J. Li, M. Ding and L. Gao, *Dalton Transactions*, 2013, **42**, 3936-3940.
33. O. Kolmykov, N. Chebbat, J.-M. Commenge, G. Medjahdi and R. Schneider, *Tetrahedron Lett*, 2016, **57**, 5885-5888.
34. K. Kida, K. Fujita, T. Shimada, S. Tanaka and Y. Miyake, *Dalton Transactions*, 2013, **42**, 11128-11135.
35. G. Lu, S. Li, Z. Guo, O. K. Farha, B. G. Hauser, X. Qi, Y. Wang, X. Wang, S. Han, X. Liu, J. S. DuChene, H. Zhang, Q. Zhang, X. Chen, J. Ma, S. C. J. Loo, W. D. Wei, Y. Yang, J. T. Hupp and F. Huo, *Nature Chemistry*, 2012, **4**, 310.
36. F. Freeman, *Chemical Reviews*, 1980, **80**, 329-350.
37. S. Pennathur, *Lab on a Chip*, 2008, **8**, 383-387.
38. T. L. Liu and C. J. Kim, *Science*, 2014, **346**, 1096-1100.
39. R. Chen, J. Kang, M. Kang, H. Lee and H. Lee, *Bulletin of the Chemical Society of Japan*, 2018, **91**, 979-990.
40. J. L. Wilbur, A. Kumar, E. Kim and G. M. Whitesides, *Advanced Materials*, 1994, **6**, 600-604.

